A METHOD TO MAP AGRICULTURAL LAND ABANDONMENT USING HIGH SPATIAL AND TEMPORAL RESOLUTION IMAGES

Yoshihiko Kobayashi (1), Tsuguki Kinoshita (2)

[1] Graduate School of Agriculture, Ibaraki Univ., 3-21-1 Chuo, Ami, Ibaraki 300-0393, Japan

[2] College of Agriculture, Ibaraki Univ., 3-21-1 Chuo, Ami, Ibaraki 300-0393, Japan
Email: 19am404t@vc.ibaraki.ac.jp; tsuguki.kinoshita.00@vc.ibaraki.ac.jp;

KEY WORDS: Japan, NDVI Time-series, Phenology, PlanetScope, Rate-of-change

ABSTRACT: Agricultural land abandonment is distributed over the world. It causes environmental and socio-economic problems. That is the reason why understanding the drivers of abandonment is essential. Monitoring agricultural land is important for that. Satellite remote sensing is one of the promising ways to understand spatial pattern of abandonment. We suggest a method to detect abandonment based on high spatial and high temporal resolution images. The fine resolution can identify small land parcels. The frequent data acquisition enables to observe vegetation dynamics. Abandonment causes characteristic Normalized Difference Vegetation Index (NDVI) change pattern, so vegetation dynamics is valuable for monitoring abandonment. The vegetation dynamics are often described using NDVI time-series. We used NDVI time-series derived from PlanetScope satellite constellation images. PlanetScope observes entire Earth's terrestrial surface every day. It has a Ground Sample Distance of 3.7 meters. In the suggested method, NDVI rate-of-change time-series was generated for each pixel firstly. Then, rule-based classification using threshold was applied. Our approach was tested in Ami-town, Ibaraki Prefecture, Japan. Input data include 16 cloud-free images acquired in April to November in 2018. When extremely abandoned agricultural land and paddy were classified, the map had an overall accuracy of 99.4%. Also, PA / UA of the abandoned class were 98.9% and 94.5%, respectively. On the other hand, when moderately abandoned agricultural land and paddy were classified, the map had an overall accuracy of 34.3%. Also, PA / UA of the abandoned class were 93.9% and 25.4%, respectively. It was likely due to homogeneity between moderately abandoned agricultural land and active one. Besides, image acquisition dates and the individual difference in sensors may have influenced our results. Our study highlighted the importance of capturing plant phenology using high spatial and temporal resolution images and can contribute to mapping abandonment spatial pattern more accurately.

1. INTRODUCTION

Agricultural land is the basis of food production and one of the vital land use. Now, abandoned agricultural land is increasing over the world. Agricultural abandonment has environmental and socio-economic consequences. For example, abandonment increases the risk of threatening food production. Therefore, understanding abandonment drivers are essential. That is why an accurate abandonment map is needed. Land use in agricultural land often changes year by year, so the annual survey is important. However, the annual survey takes much effort, so reliable spatial data of abandonment is missing. Remote sensing using satellite images can capture vegetation cover widely. Therefore, remote sensing has been used for detecting abandonment (Alcantara et al., 2012; Dara et al., 2018; Estel et al., 2015; Fukumoto and Yoshisako, 2014; Kato et al., 2003; Löw et al., 2015; Yin et al., 2018; Zukemura et al., 2011). The past effort has used multi-temporal satellite data from MODIS (Alcantara et al., 2012; Estel et al., 2015), Landsat (Dara et al., 2018; Löw et al., 2015; Yin et al., 2018), RapidEye (Fukumoto and Yoshisako, 2014; Löw et al., 2015), ALOS/AVNIR2 (Fukumoto and Yoshisako, 2014; Zukemura et al., 2011) and SPOT (Kato et al., 2003). Some studies have used coarser resolution images such as MODIS. That is because MODIS has a high temporal resolution due to the wide swath width. High temporal resolution images can capture gradual processes of abandonment. In other words, temporally high resolution images can detect the phenological profile of abandoned and active agricultural land. Besides, it is easy to get cloud-free images. However, it was potentially limiting because coarser resolution images cannot capture the complexity of smaller agricultural lands. On the other hand, spatially middle or high resolution satellite images such as Landsat/ETM+ and RapidEye can capture smaller parcels. Finer resolution may offer advantages on the mapping of the complex area. However, these have a lower temporal resolution, and image availability is lower than coarser resolution sensors. Generally, a high temporal resolution sensor has a low spatial resolution. In contrast, a middle or high spatial resolution sensor has a low temporal resolution. The satellite constellation is one way to solve the problem. When a lot of small satellites consist an observation network, high temporal resolution and high spatial resolution can be compatible. PlanetScope is a constellation of nanosatellite manufactured by Planet. It consists of more than 120 CubeSat named Dove. Also, PlanetScope acquires entire Earth's images every day with 3.7m Ground Sample Distance (GSD) (Planet Labs, 2018).

Therefore, we can conduct land use detection using high spatial and temporal resolution images. It provides an opportunity for mapping abandonment accurately.

Two methods have been used to map abandonment in the existing literature. First is an analysis of the land use trajectory (Löw et al., 2015). This method uses the inter-annual land use change pattern to detect abandonment. So, the trajectory-based approach uses multi-year satellite data. Similarly, another trajectory-based change detection approach is suggested (Dara et al., 2018; Yin et al., 2018). This approach uses agricultural land probability time-series. The probability is derived from satellite images for each year using random forest (Dara et al., 2018; Yin et al., 2018). The second approach is based on the Normalized Difference Vegetation Index (NDVI) seasonal change (Fukumoto and Yoshisako, 2014; Kato et al., 2003; Zukemura et al., 2011). NDVI is a satellite-based vegetation index. It correlates strongly with aboveground net primary productivity (Pettorelli et al., 2005). These approaches focus on NDVI signature within a year. Active agricultural land has a characteristic phenological signature. It corresponds to farm operations such as planting and harvesting. NDVI of active agricultural land becomes low because of plowing. NDVI then becomes high in summer according to growing. Lastly, harvesting in autumn causes a drop of NDVI. In other words, active agricultural land has characteristic NDVI pattern. On the other hand, abandoned agricultural lands do not have plowing and harvesting season. Therefore, depending on the differences in phenology, we can separate abandoned agricultural land from the active one. Not only NDVI value itself but also phenology metrics derived from NDVI are used for abandonment mapping (Alcantara et al., 2012). For example, one study used eleven phenology metrics: start, end, length, middle and amplitude of the growing period, NDVI base level, maximum NDVI, rate of increase and decrease, and growing period integral (Alcantara et al., 2012). However, in the past studies, NDVI rate-of-change time-series is rarely used for a mapping abandonment. Rate-of-change could detect rapid NDVI change corresponding to the farm operation. It is not clear that the NDVI rate of change analysis works on abandonment detection. Therefore, our research focused on the discrimination of abandoned and active agricultural land based on NDVI rate-of-change time-series. Besides, we aimed to find a combination of classes which can be discriminative using phenological information.

2. METHOD

2.1 Study area

We tested our approach in Ami-town, Ibaraki Prefecture, Japan. Ami-town is the area on the Pacific side and located in the south of Lake Kasumigaura. In Ami-town, agricultural land abandonment has been widely occurring. The rate of abandonment was 36.84% in 2015. It is higher than the average rate in Japan (12.14%). The topography is relatively flat and above mean sea level is 21m. (Ami-town office, 2015a). The climate is characterized by rain from June to July, and the amounts of snow are small in winter. Monthly precipitation ranges from 12mm to 257mm (Ami-town Office, 2015b). Average temperatures in June is 19.6 degrees Celsius (Ami-town Office, 2015b). In farmlands, area of rice is the largest, and green onion and Chinese cabbage follow (MAFF, 2015). Figure 1 shows the study area. It covers about 12 km^2.
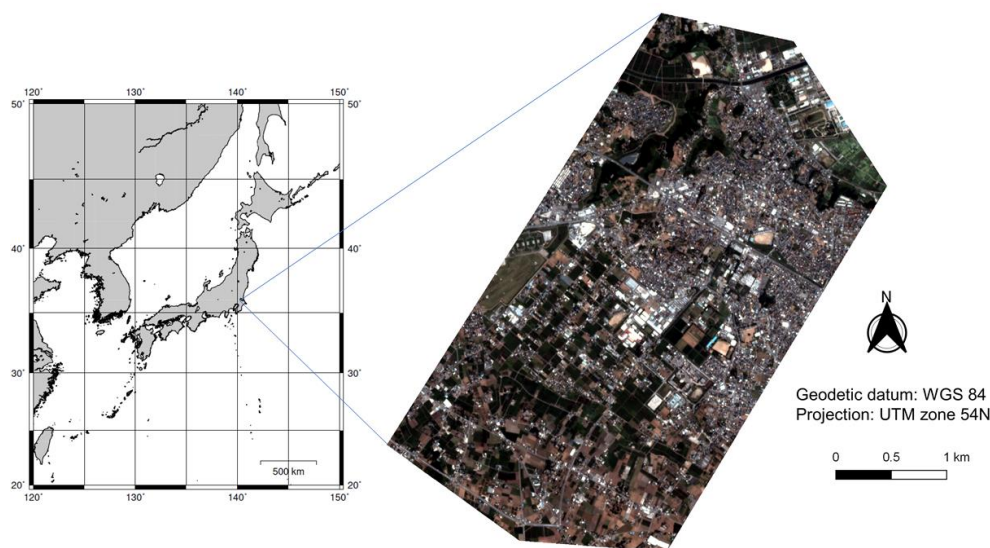
Figure 1 Location of the study region in Ami-town, Ibaraki Prefecture, Japan (PlanetScope analytic surface reflectance product acquired in 2018/07/02 is shown as R = Band3, G = Band2, B = Band1)

2.2 Data

Input data for the classifications

We used the 4-band PlanetScope images (Planet Team, 2017). Each PlanetScope satellite is a CubeSat 3U form factor (10 cm by 10 cm by 30 cm) (Planet Labs, 2018). The complete PlanetScope constellation of approximately 130 satellites can image the entire land surface of the Earth every day (equating to a daily collection capacity of 200 million km²/day) (Planet Labs, 2018). Table 1 shows PlanetScope specification. We used the 4-band PlanetScope images from April 13, 2018, to November 2, 2018. In other words, we used images between DOY 103 and 306. These include 16 cloud-free (cloud cover 0 - 1%) images. When one scene cannot cover the whole range in our study area, two images with a 1-second difference in shooting time were combined and used. Six images were combined into three scenes, so 16 scenes derived from 19 images were finally used. The data type of these images is unsigned integer 16 bits. Data were retrieved from Planet.com on May 28, 2019. The following is the list of used images (Table 2).

Table 1 PlanetScope constellation and sensor specifications based on (Planet Labs, 2018)

Mission Characteristics	Sun-synchronous Orbit
Orbit Altitude (reference)	475 km (~98° inclination)
Max/Min Latitude	±81.5° (depending on season)
Equator Crossing Time	9:30 - 11:30 am (local solar time)
Sensor Type	Three-band frame Imager or four-band frame Imager with a split-frame NIR filter
Spectral Bands	Blue: 455 - 515 nm Green: 500 - 590 nm Red: 590 - 670 nm NIR: 780 - 860 nm
Ground Sample Distance (nadir)	3.7 m
Frame Size	24.6 km x 16.4 km (approximate)
Maximum Image Strip per orbit	20,000 km²
Revisit Time	Daily at nadir (early 2017)
Image Capture Capacity	200 million km²/day
Camera Dynamic Range	12-bit

Table 2 PlanetScope images used for classification

No.	ID	Acquisition date	DOY	Cloud cover	Same date
1	20180413_004938_0f17	2018/04/13	103	0-1%	
2	20180420_004949_101d	2018/04/20	110	0-1%	
3	20180429_010338_0f46	2018/04/29	119	0-1%	
4	20180505_005112_0f15	2018/05/05	125	0-1%	
5	20180511_005039_1005	2018/05/11	131	0-1%	
6	20180516_010130_0f4d 20180516_010131_0f4d	2018/05/16	136	0-1%	○
7	20180522_005019_1033	2018/05/22	142	0-1%	
8	20180603_005124_0f25 20180603_005125_0f25	2018/06/03	154	0-1%	○
9	20180702_005457_0f3c	2018/07/02	183	0-1%	
10	20180801_005316_1034	2018/08/01	213	0-1%	
11	20181002_005438_1029	2018/10/02	275	0-1%	
12	20181007_005609_0f4e	2018/10/07	280	0-1%	
13	20181022_005540_1014	2018/10/22	295	0-1%	
14	20181025_003709_1051	2018/10/25	298	0-1%	
15	20181030_005105_0e2f	2018/10/30	303	0-1%	
16	20181102_005601_1022 20181102_005603_1022	2018/11/02	306	0-1%	○

Class setting

Table 3 shows seven classes for classification. Abandoned and active agricultural land were set. Abandoned agricultural land was separated into three classes: Abandoned (tree), Abandoned (herbaceous) and Abandoned (managed). Active agricultural land was separated into four classes: Field, Tree nursery, Paddy, and Rikuden.

Paddy indicates a paddy field for rice. Rikuden also indicates land used for rice production even though Rikuden is not registered as a paddy field but as cropland. The difference depends on the administrative category of land use. Because of within-class heterogeneity, Abandoned (managed) and Field were excluded from the subsequent classification. Because of homogeneity between Paddy, and Rikuden and homogeneity between Abandoned (tree) and Tree nursery, Rikuden and Tree nursery was also excluded from the subsequent classification. Finally, Abandoned (herbaceous), Abandoned (tree) and Paddy class is used for classification.

Table 3 Class and definition

No.	Class	Definition
1	Abandoned (herbaceous)	Abandoned agricultural land where herbaceous plants grow
2	Abandoned (tree)	Abandoned agricultural lands where herbaceous plants and woody plants grow
3	Abandoned (managed)	Abandoned agricultural land where herbaceous plants grow however, these are cut regularly
4	Paddy	Paddy fields for rice
5	Rikuden	Agricultural lands for rice where are registered as cropland
6	Field	Cropland
7	Tree nursery	Agricultural lands where trees for sales grow
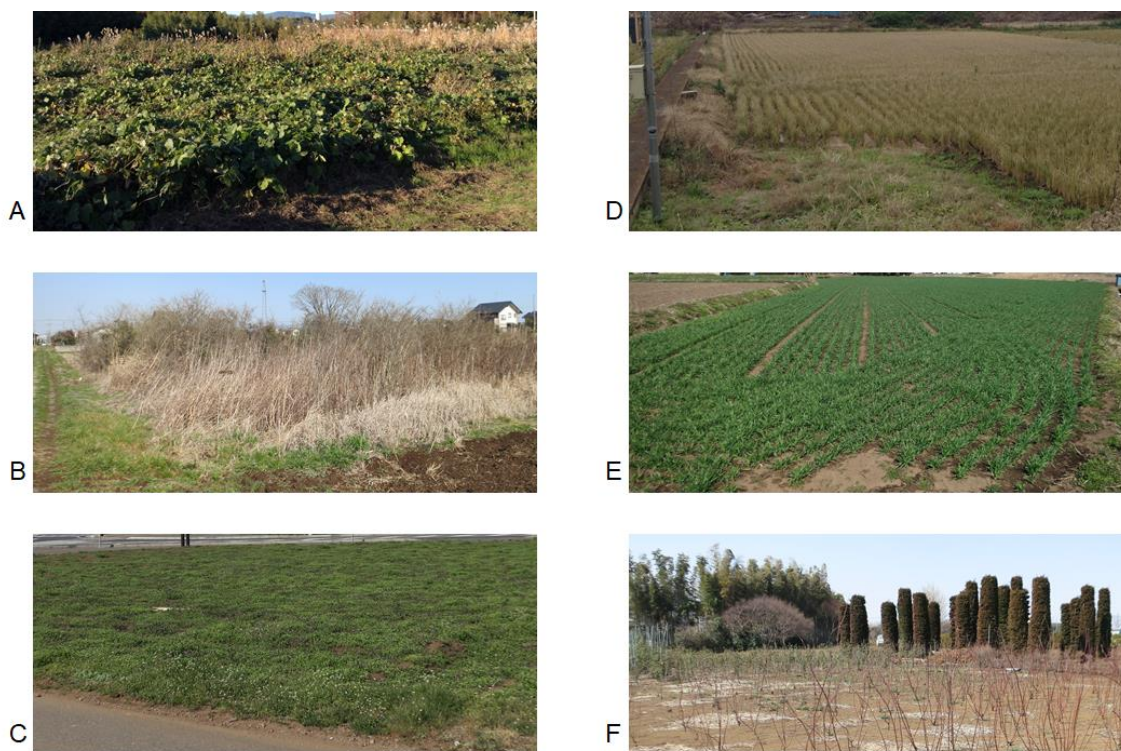
Figure 2 Agricultural land use categories sampled in Ami-town A: Abandoned (herbaceous), B: Abandoned (tree), C: Abandoned (managed), D: Paddy and Rikuden, E: Field, F: Tree nursery

Parcel polygon and training/validation data

In this study, the two-class classification was conducted. For class-wise analysis, satellite images were clipped using the parcel polygons for each class. The parcel polygon was generated based on field observation. We conducted the field survey in November 2018, December 2018, and March 2019. For further correctness, false-color satellite images and high-resolution aerial photographs in Google Earth™ were used. These images were interpreted visually, and problematic data such as too small polygon and mixed polygon were deleted. Figure 3 shows the PlanetScope images in Ami-town and the parcel polygons. For class-wise analysis, images were clipped using parcel polygons for each class. Then, simple random sampling was applied for the data partition. In other words, all data in each class were equally separated into training and validation data randomly. Table 4 shows the numbers of training and validation data.
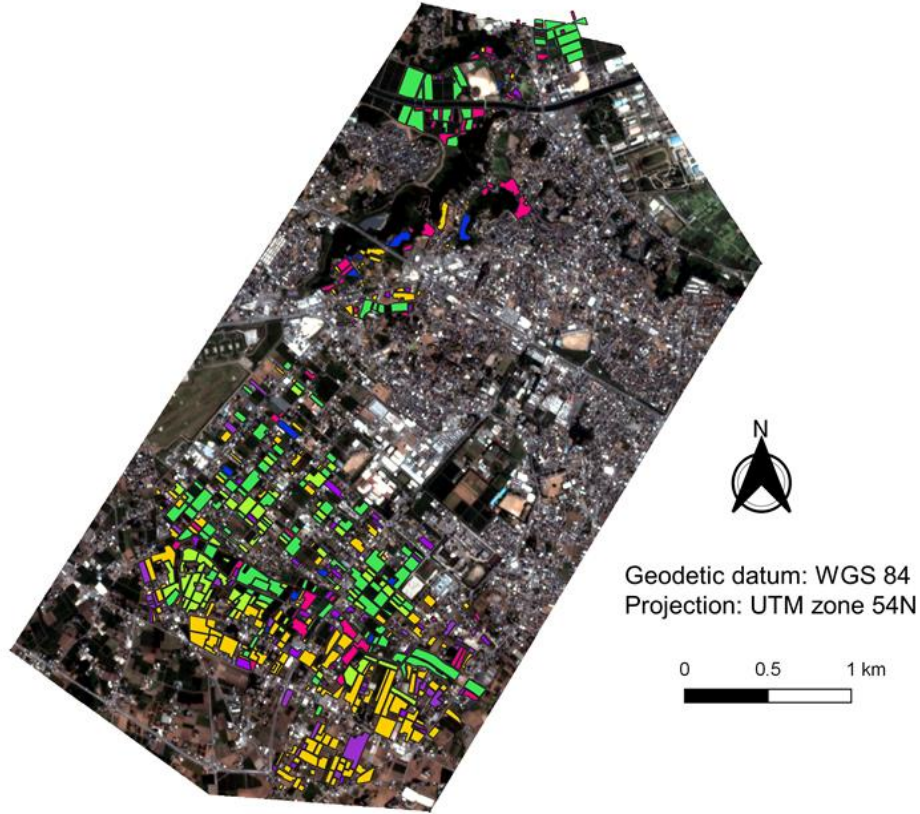
**Figure 3 Agricultural land parcel polygons overlaid on PlanetScope image
(2 July 2018, shown as RGB = Band3, Band2, Band1) in the study area**

Table 4 Numbers of training and validation pixel in each class (Unit: Pixel)

Class	Total	Training	Validation
Abandoned (herbaceous)	12377	6189	6188
Abandoned (tree)	3780	1890	1890
Paddy	40841	20421	20420

2.3 Classification workflow

Firstly, images were clipped by parcel polygons of each class. As a result, class-wise images were generated. These were transformed into ASCII numerical data using ENVI Classic 5.4 (ESRI). NDVI was calculated using the following formula (Pettorelli et al., 2005) for each pixel.

$$NDVI = \frac{NIR - RED}{NIR + RED}, \tag{1}$$

where NIR and RED are spectral reflectance in red (Band 3) and spectral reflectance in near-infrared (Band 4), respectively. As a result, NDVI time-series were generated for each class. Data were smoothed to reduce noises. In other words, a simple average of two adjacent observation data was applied twice. As a result, 14 smoothed observation data was generated. That is because of information loss according to average iteration. Cubic spline interpolation (Mckinley and Levine, 1998) was applied to fill data in the missing dates. In cubic spline interpolation, a series of unique cubic polynomials are fitted between each of the data points, with the stipulation that the curve obtained be continuous and appear smooth (Mckinley and Levine, 1998). As a result, daily NDVI data in DOY = 111 to 302 was generated for each class. Then, the NDVI rate-of-change was calculated using finite differences. The following fourth-order formula (Moin, 2010) is used for the calculation.

$$f_j' = \frac{f_{j-2} - 8f_{j-1} + 8f_{j+1} - f_{j+2}}{12h} + O(h^4), \tag{2}$$

where h is mesh size, f_j' indicates the approximation for the derivative of $f(x)$ at the point x_j and $O(h^4)$ indicates the order of accuracy. As a result, NDVI rate-of-change in DOY = 113 to 300 (188 days) were

generated. The data was partitioned to training data and validation data. For the classification, rule-based classification method using threshold (Maxwell and Sylvester, 2012) was chosen. The threshold values were set based on visual interpretation of training data. Validation data were classified by the pre-defined threshold. Then, overall, producer's, and user's accuracy (Russell G. Congalton, 1999) were calculated. Figure 4 shows the classification flow.
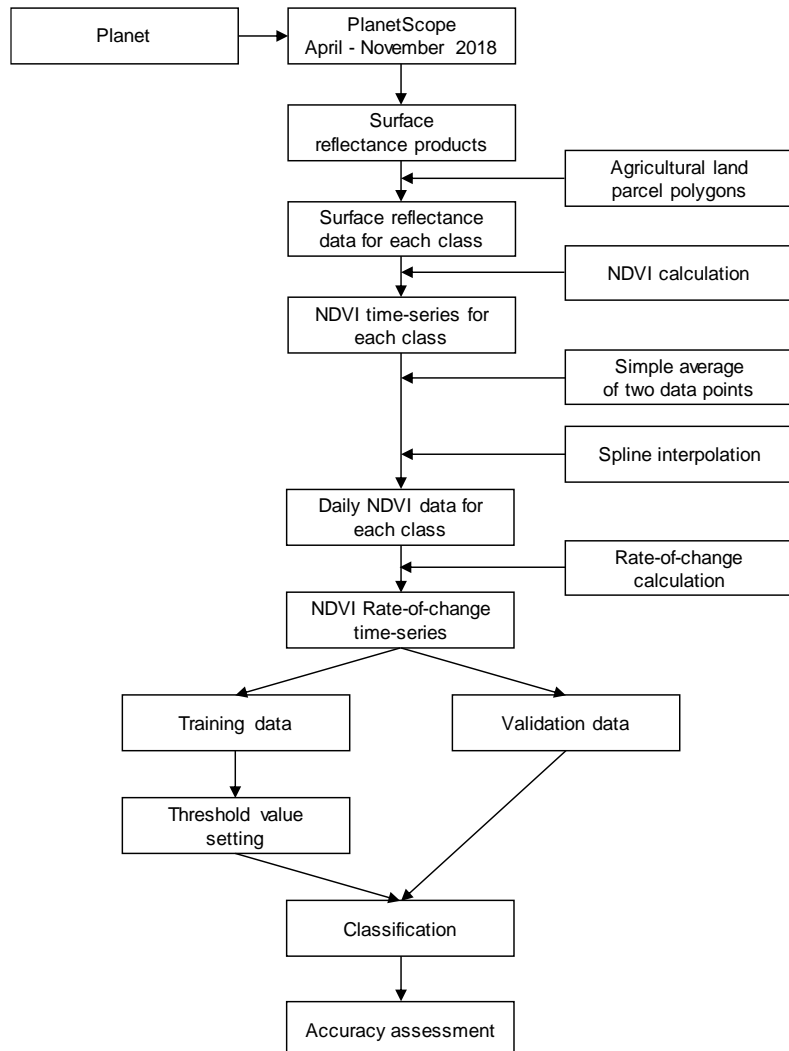
Figure 4 Flowchart depicting the major steps to detect abandoned agricultural land

3. RESULTS AND DISCUSSION

3.1 NDVI time-series and phenological profiles

Figure 5, Figure 6, and Figure 7 show NDVI time-series of Abandoned (herbaceous), Abandoned (tree) and Paddy. Each NDVI time-series reflects the phenological profile of each class. Abandoned (tree) had the smallest intraclass variation (Figure 6). Besides, the rate-of-change in Abandoned (tree) was almost 0.00 in around DOY = 150 to 280. That is because woody plants have consistent vegetation activity throughout the year, and it appeared as low rate-of-change. On the other hands, Paddy had a larger intraclass variation according to pixels. Besides, the rate-of-change in Paddy changed depending on the season. The rate-of-change takes a positive value up to DOY = 140-200 (Figure 7). After that, in DOY = 200 to 260, the rate-of-change takes a negative value. The negative value would have reflected the growth and ripening processes of paddy rice. The difference between Abandoned (tree) and Paddy lies in around DOY = 160. Paddy has a positive rate-of-change, even though Abandoned (tree) has almost zero of rate-of-change (Figure 6, Figure 7). Because of the difference, it is easy to distinguish the Paddy from Abandoned (tree). However, it is more challenging to distinguish Paddy from Abandoned (herbaceous). That is because Paddy and Abandoned (herbaceous) have a similar pattern over the year. The small difference between Paddy and Abandoned (herbaceous) is the absolute value of rate-of-change. Paddy has a higher rate-of-change absolute value around DOY = 280-300 (Figure 7) compared with Abandoned (herbaceous).

Rate of change value in Paddy is sometimes more than 0.005. On the other hands, Abandoned (herbaceous) does not have a rate-of-change absolute value exceeding 0.005 (Figure 5). The difference in change rate value may be because of harvesting. Because harvesting is performed in Paddy, the rate-of-change may swing significantly negative to less than -0.01. Harvesting is not performed in Abandoned (herbaceous), so the amount of plants does not change, and rate-of-change absolute value kept low.
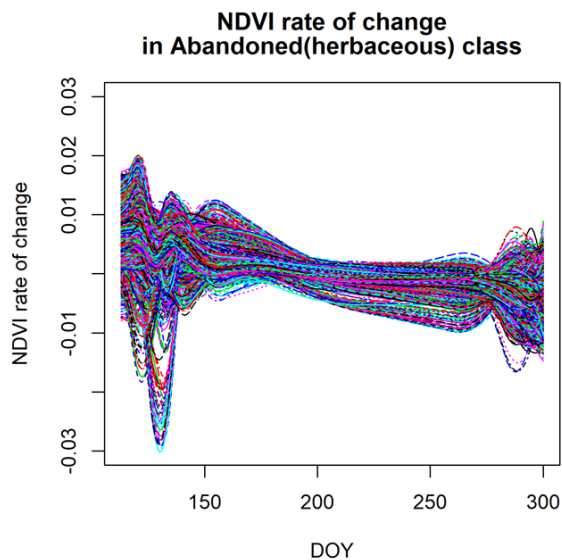
Figure 5 NDVI rate-of-change of all 6189 pixels in Abandoned(herbaceous)
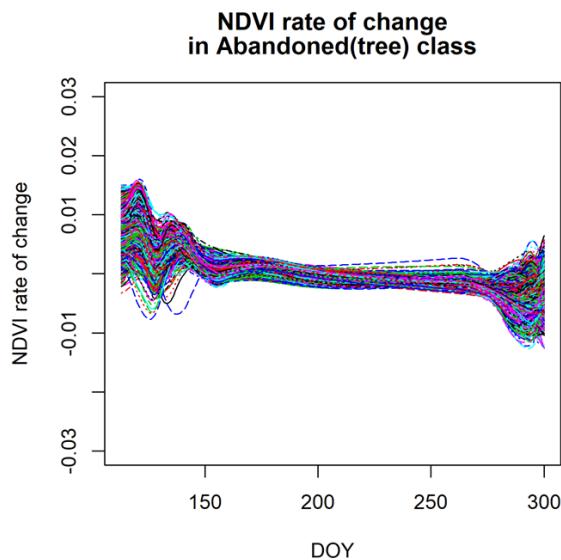
Figure 6 NDVI rate-of-change of 1881 pixels in Abandoned(tree)
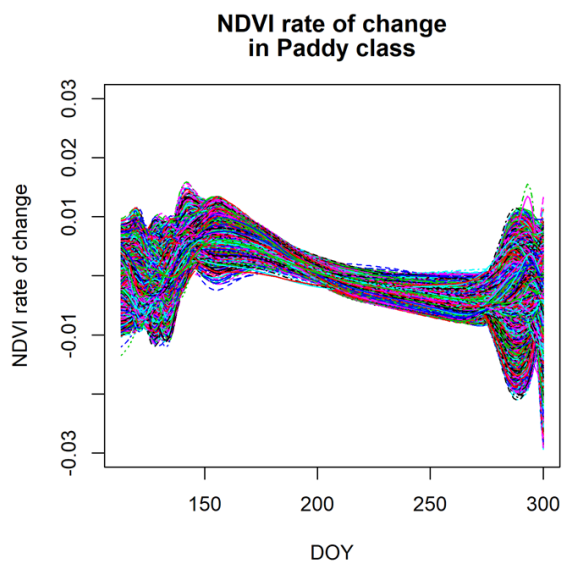
Figure 7 NDVI rate-of-change of 20409 pixels in Paddy

3.2 Threshold setting

We found substantial differences between Abandoned (tree) and Paddy. As a threshold, we used NDVI rate-of-change absolute value at the beginning of the growing season and harvesting season. Each of Abandoned (tree) and Abandoned (herbaceous) is classified against Paddy. When we classify Abandoned (tree) and Paddy, if the absolute value of rate-of-change is smaller than 0.003 at DOY=158, it is classified as Abandoned (tree). When we classify Abandoned (herbaceous) and Paddy, if the absolute value of rate-of-change is smaller than 0.005 at DOY=283, it is classified as Abandoned (herbaceous).

3.3 Agricultural land abandonment map and performance
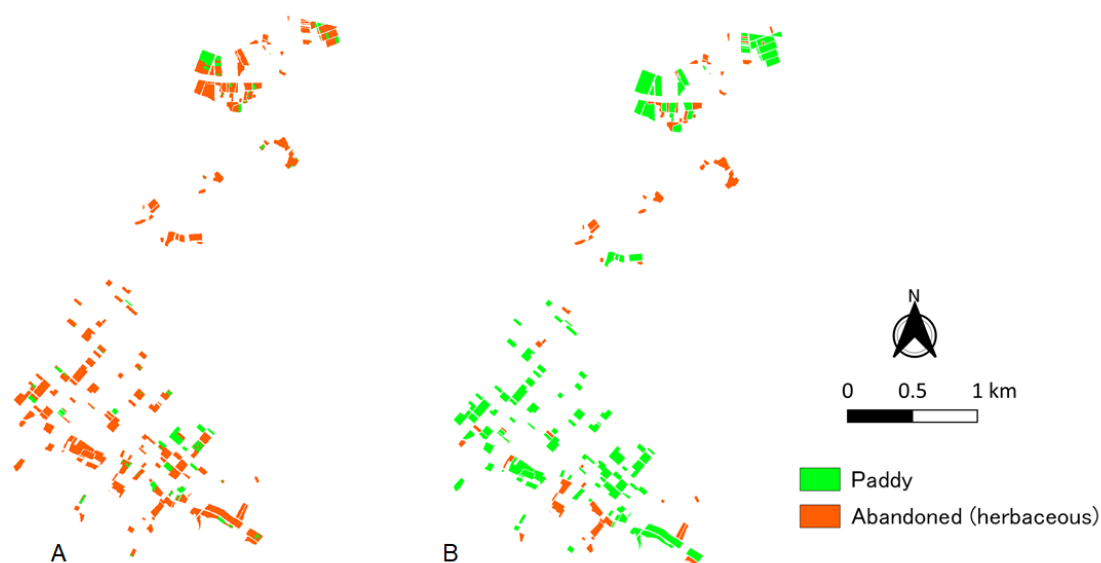
Figure 8 Classification result of Paddy vs. Abandoned (herbaceous)
A: Classified result, B: Reference parcel polygon
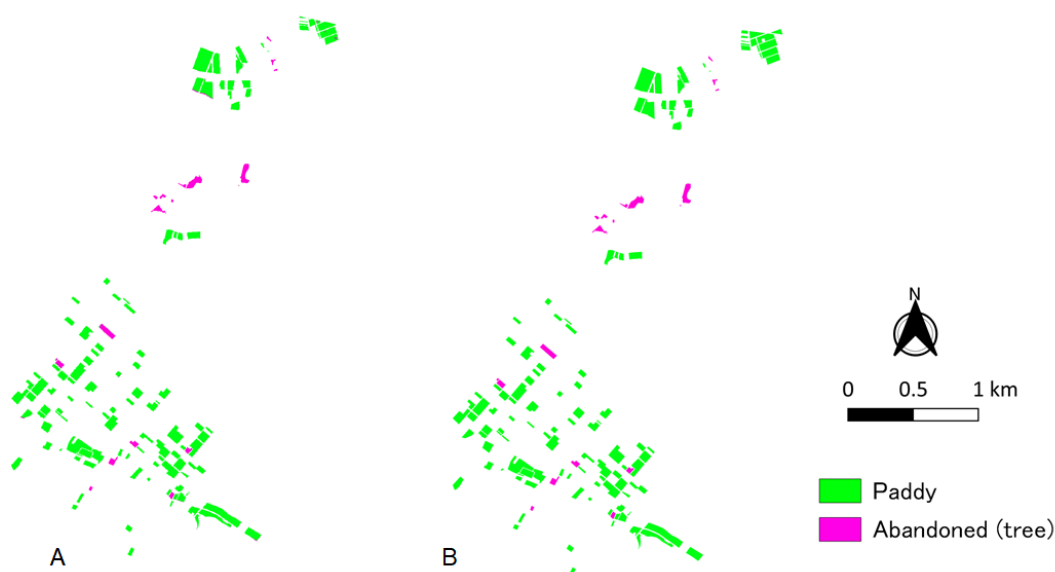
Figure 9 Classification result of Paddy vs. Abandoned (tree)
A: Classified result, B: Reference parcel polygon

Figure 8 and Figure 9 show the two classification results of Paddy vs. Abandoned (herbaceous), and Paddy vs. Abandoned (tree). The overall accuracy of the Abandoned agricultural land ranged from 34.3% to 99.4% (Table 5, Table 6). The two classification results showed contrasting classification accuracy according to the degree of abandonment. When Abandoned (tree) and Paddy was classified, our test showed the best accuracy. When Abandoned (herbaceous) and Paddy was classified, our test showed the worst accuracy. The differences between Abandoned (herbaceous) and Abandoned (tree) is the existence of trees.

In the Abandoned (tree) against Paddy classification, the overall accuracy was 99.4% (Table 6). In this classification, Abandoned (tree) had a producer's accuracy of 98.9% and user's accuracy of 94.5 %. In the Abandoned (herbaceous) against Paddy classification, the overall accuracy was 34.3% (Table 5). In this classification, Abandoned (herbaceous) had a producer's accuracy of 93.9% and a user's accuracy of 25.4%. Table 7 and Table 8 shows confusion matrixes of the two classifications. A lot of pixels belong to Paddy was misclassified as Abandoned (herbaceous) (Table 8). The main reason for the confusion is the similarity of these

two class in NDVI pattern. The results showed that trees have more characteristic NDVI pattern.

Table 5 Accuracy of Abandoned (herbaceous) vs. Paddy

	Unit: %
OA	34.3
PA [Abandoned (herbaceous)]	93.9
PA [Paddy]	16.2
UA [Abandoned (herbaceous)]	25.4
UA [Paddy]	89.8

Table 6 Accuracy of Abandoned (tree) vs. Paddy

	Unit: %
OA	99.4
PA [Abandoned (tree)]	98.9
PA [Paddy]	99.5
UA [Abandoned (tree)]	94.5
UA [Paddy]	99.9

Table 7 Confusion matrix of Abandoned (herbaceous) vs. Paddy

Unit: Pixel	Ground Truth	
	Abandoned (herbaceous)	Paddy
Abandoned (herbaceous)	5813	17109
Paddy	375	3311

Table 8 Confusion matrix of Abandoned (tree) vs. Paddy

Unit: Pixel	Ground Truth	
	Abandoned (tree)	Paddy
Abandoned (tree)	1869	108
Paddy	21	20312

3.4 General trends

Our results showed that the NDVI rate of change is suitable to identify the agricultural land abandonment with woody plants from the paddy field. Our validation data showed that our approach could map extremely abandoned agricultural land. That was because NDVI rate-of-change of Abandoned (tree) was often much smaller than that of active agricultural land. On the other hands, the Abandoned (herbaceous) was difficult to detect. The similarity in NDVI pattern between Abandoned (herbaceous) and Paddy caused classification errors. In other words, we could not have found the big difference between Abandoned (herbaceous) and Paddy in the NDVI rate-of-change time-series. Therefore, we could not have set the appropriate threshold. Heterogeneity within each class was large, and phenological profile of active agricultural land was similar to that of abandoned agricultural land. Also, the mapping of abandonment became challenging because of the variability in pixels of each class.

3.5 Uncertainty and limitations

Firstly, in this study, satellite images for the period from April 2018 to November 2018 were used. On the other hand, we conducted a field survey from November 2018 to March 2019. Survey dates were winter in Japan, and sometimes cropland was covered by weed with a low height. So, the error of class label judgment could have occurred. In particular, the abandoned agricultural land parcel polygon is likely less reliable. That is because weeds in abandoned agricultural land die in winter and it makes judgment difficult. Secondly, the influence of image availability may have been strong. Even though we used high temporal resolution images, the observation frequency of each season was not equal. Most of the images from June to September was not available because of the rainy season in this area. Therefore, we could have not captured the NDVI characteristics in the growing season accurately. Because data were smoothed by taking an average, if the acquisition interval was wide, smoothing might make a failure. Also, the reliability of data interpolated from the smoothed data could have decreased. Thirdly, PlanetScope images were acquired by different sensor every time. These sensors have slightly different conditions and characteristics. Besides, a different atmospheric condition in each season could have influenced the images. As shown in Figure 5 and Figure 7, NDVI rate-of-change strongly varied for pixels. Even though pixels were adjacent, sometimes rate-of-change was different. It was likely due to noises originated from the difference between sensors and atmospheric condition variation. Smoothing relaxed the condition, but it

could have been not sufficient. Fourth, we tested our approach in a temperate humid climate area. In our study area, more than half of the agricultural lands are used for rice paddy. Also, we conducted classification in terms of abandoned agricultural land and paddy field. It suggests that our method could be transferred only into the rice-producing district. In addition, because single-crop is conducted in this region, the adjustment may be needed in the area the double-cropping is conducted.

4. CONCLUSION

Our research focused on the NDVI rate-of-change time-series derived from high spatial and temporal satellite images. Our goal was to discriminate abandoned and active agricultural land based on NDVI seasonal change. Available PlanetScope images successfully distinguished extremely abandoned and paddy field. On the other hand, the accuracy was limited when the degree of abandonment was not so high. Therefore, when extremely abandoned agricultural land and paddy field are classified, the proposed method may be useful. Our study can lead to a deeper understanding of spatial pattern and drivers of abandonment.

REFERENCES

Alcantara, C., Kuemmerle, T., Prishchepov, A. V., Radeloff, V.C., 2012. Mapping abandoned agriculture with multi-temporal MODIS satellite data. Remote Sens. Environ. 124, pp. 334–347.
Ami-town Office, 2015a. Location and topography of Ami-town, Retrieved July 18, 2019, from https://www.town.ami.lg.jp/0000000991.html.
Ami-town Office, 2015b. The climate of Ami-town, Retrieved July 18, 2019, from http://www.town.ami.lg.jp/0000000992.html.
Dara, A., Baumann, M., Kuemmerle, T., Pflugmacher, D., Rabe, A., Griffiths, P., Hölzel, N., Kamp, J., Freitag, M., Hostert, P., 2018. Mapping the timing of cropland abandonment and recultivation in northern Kazakhstan using annual Landsat time series. Remote Sens. Environ. 213, pp. 49–60.
Estel, S., Kuemmerle, T., Alcántara, C., Levers, C., Prishchepov, A., Hostert, P., 2015. Mapping farmland abandonment and recultivation across Europe using MODIS NDVI time series. Remote Sens. Environ. 163, pp. 312-325.
Fukumoto, M., Yoshisako, H., 2014. Screening Method of Paddy Fields Targeted for Field Surveys during Investigations on the Status of Generation and Elimination of Devastated Farmlands Using Multitemporal Satellite Data and Paddy Parcel Boundary Data. Trans. Japanese Soc. Irrig. Drain. Rural Eng. 82, pp. 339-346 (in Japanese).
Kato, J., Uehara, Y., Tanimoto, T., 2003. Distinction of Devastated Paddy Fields Using Satellite Data. J. Remote Sens. Soc. Japan 23, pp. 550-554 (in Japanese).
Löw, F., Fliemann, E., Abdullaev, I., Conrad, C., Lamers, J.P.A., 2015. Mapping abandoned agricultural land in Kyzyl-Orda, Kazakhstan using satellite remote sensing. Appl. Geogr. 62, pp. 377–390.
MAFF, 2015. Statistics Ami-town fundamental data, Retrieved July 19, 2019, from http://www.machimura.maff.go.jp/machi/contents/08/443/index.html.
Maxwell, S.K., Sylvester, K.M., 2012. Identification of "ever-cropped" land (1984-2010) using Landsat annual maximum NDVI image composites: Southwestern Kansas case study. Remote Sens. Environ. 121, pp. 186–195.
Mckinley, S., Levine, M., 1998. Cubic spline interpolation. Coll. Redwoods 45, pp. 1049–1060.
Moin, P., 2010. Fundamentals of engineering numerical analysis. Cambridge University Press, pp. 13-15.
Pettorelli, N., Vik, J.O., Mysterud, A., Gaillard, J.M., Tucker, C.J., Stenseth, N.C., 2005. Using the satellite-derived NDVI to assess ecological responses to environmental change. Trends Ecol. Evol. 20, pp. 503–510.
Planet Team, 2017. Planet Application Program Interface: In Space for Life on Earth. San Francisco, CA. Retrieved May 28, 2019, from https://api.planet.com.
Planet Labs, 2018. Planet Imagery Product Specifications, Retrieved July 26, 2019, from https://assets.planet.com/docs/Planet_Combined_Imagery_Product_Specs_letter_screen.pdf.
Russell G. Congalton, K.G., 1999. Assessing the accuracy of remotely sensed data Principles and Practices. CRC Press.
Yin, H., Prishchepov, A. V., Kuemmerle, T., Bleyhl, B., Buchner, J., Radeloff, V.C., 2018. Mapping agricultural land abandonment from spatial and temporal segmentation of Landsat time series. Remote Sens. Environ. 210, pp. 12–24.
Zukemura, C., Motohka, T., Nasahara, K., 2011. Detection of Abandoned Rice Paddies with Satellite Remote Sensing. J. Remote Sens. Soc. Japan 31, pp. 55-62 (in Japanese).